

## Supporting Information

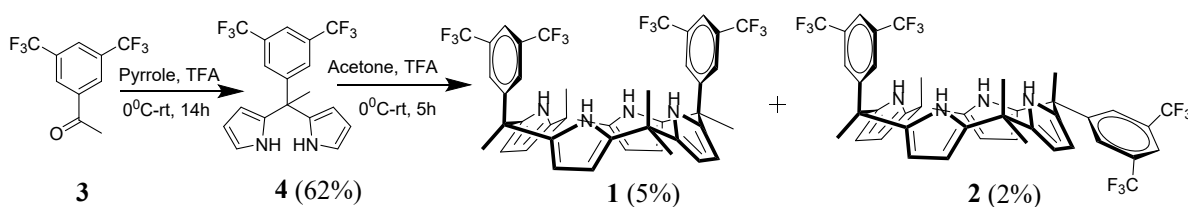
Table of content	Page no.
<b>Section S1.</b> General information and instrumentations.	2
<b>Section S2.</b> Experimental section: synthetic scheme and synthetic procedures.	3
<b>Fig. S1.</b> <sup>1</sup> H NMR spectrum of <b>4</b> .	4
<b>Fig. S2.</b> <sup>13</sup> C NMR spectrum of <b>4</b> .	5
<b>Fig. S3.</b> HRMS spectrum of <b>4</b> .	6
<b>Fig. S4.</b> <sup>1</sup> H NMR spectrum of <b>1</b> .	7
<b>Fig. S5.</b> <sup>13</sup> C NMR spectrum of <b>1</b> .	8
<b>Fig. S6.</b> HRMS spectrum of <b>1</b> .	9
<b>Fig. S7.</b> <sup>1</sup> H NMR spectrum of <b>2</b> .	10
<b>Fig. S8.</b> <sup>13</sup> C NMR spectrum of <b>2</b> .	11
<b>Fig. S9.</b> HRMS spectrum of <b>2</b> .	12
<b>Fig. S10.</b> Single crystal X-ray structures of <b>1</b> •CH <sub>2</sub> Cl <sub>2</sub> and <b>2</b> •(CH <sub>3</sub> OH) <sub>2</sub> .	13
<b>Fig. S11.</b> Single crystal X-ray structure of <b>1</b> •TBAF•H <sub>2</sub> O complex and partial view of the 1D linear supramolecular chain seen in the crystal lattice.	13
<b>Fig. S12.</b> Single crystal X-ray structure of <b>1</b> •TBACl•H <sub>2</sub> O complex and partial view of the 1D linear supramolecular chain seen in the crystal lattice.	13
<b>Fig. S13.</b> Single crystal X-ray structure of <b>1</b> •TBABr•CH <sub>3</sub> OH complex and partial view of the 1D linear supramolecular chain seen in the crystal lattice.	14
<b>Fig. S14.</b> Single crystal X-ray structure of <b>1</b> •TBAI•H <sub>2</sub> O complex and partial view of the 1D linear supramolecular chain seen in the crystal lattice.	14
<b>Table S1:</b> Selected distances in the single crystal X-ray structures of fluoride, chloride, bromide, and iodide complexes of <b>1</b> .	15
<b>Fig. S15.</b> Partial <sup>1</sup> H NMR spectra of <b>1</b> recorded in the presence and absence of ca. 5.0 equivalent amounts of TBAX (X = F <sup>-</sup> , Cl <sup>-</sup> , Br <sup>-</sup> and I <sup>-</sup> ) in CDCl <sub>3</sub> .	16
<b>Fig. S16.</b> Partial <sup>1</sup> H NMR spectra of <b>2</b> recorded in the presence and absence of ca. 5.0 equivalent amounts of TBAX (X = F <sup>-</sup> , Cl <sup>-</sup> , Br <sup>-</sup> and I <sup>-</sup> ) in CDCl <sub>3</sub> .	17
<b>Table S2.</b> Association constant values (K <sub>a</sub> in M <sup>-1</sup> ) and thermodynamic parameters for the interaction of receptors <b>1</b> and <b>2</b> with fluoride and chloride anions (as their tetrabutylammonium salts) in CH <sub>3</sub> CN measured by isothermal titration calorimetry at 298 K.	17
<b>Fig. S17.</b> ITC plots showing titrations of receptor <b>1</b> (initial concentrations: 1.39 mM) with TBAF (17.03 mM) in CH <sub>3</sub> CN at 298 K.	18
<b>Fig. S18.</b> ITC plots showing titrations of receptor <b>1</b> (initial concentrations: 1.33 mM) with TBACl (15.11 mM) in CH <sub>3</sub> CN at 298 K.	19
<b>Fig. S19.</b> ITC plots showing titrations of receptor <b>2</b> (initial concentrations: 1.45 mM) with TBAF (17.43 mM) in CH <sub>3</sub> CN at 298 K.	20
<b>Fig. S20.</b> ITC plots showing titrations of receptor <b>2</b> (initial concentrations: 1.45 mM) with TBACl (17.39 mM) in CH <sub>3</sub> CN at 298 K.	20
<b>Section S3.</b> Experimental details for single crystal X-ray structure determination.	20
<b>Table S3.</b> Selected crystal data and refinement parameters for receptor <b>1</b> •CH <sub>2</sub> Cl <sub>2</sub> and <b>2</b> •(CH <sub>3</sub> OH) <sub>2</sub> .	21
<b>Table S4.</b> Selected crystal data and refinement parameters for <b>1</b> •TBAF•H <sub>2</sub> O and	22

<b>1•TBACl•H<sub>2</sub>O.</b>	
<b>Table S5.</b> Selected crystal data and refinement parameters for <b>1•TMABr•CH<sub>3</sub>OH</b> and <b>1•TMAI•H<sub>2</sub>O.</b>	23
<b>Section S4.</b> Experimental section for anion transport studies.	23
<b>Fig. S21.</b> Schematic representation of transmembrane anion transport activity studies using ion-selective electrode (A). Concentration-dependent valinomycin-coupled Cl <sup>-</sup> ion efflux studies of receptor <b>1</b> in the presence of valinomycin (B). Temperature-dependent valinomycin-coupled F <sup>-</sup> ion efflux studies of receptor <b>1</b> across DPPC bilayers (C). Time-dependent F <sup>-</sup> ion transport study of receptor <b>1</b> across the U-tube (D).	27
<b>Fig. S22.</b> Concentration-dependent F <sup>-</sup> ion efflux studies of receptor <b>1</b> in the absence of valinomycin. LUVs were prepared in 10 mM HEPES buffer containing 300 mM KF at pH 7.2 and suspended in 10 mM HEPES buffer containing 300 mM KGlc at pH 7.2 (A). Analysis of valinomycin-coupled F <sup>-</sup> ion efflux efficiency of receptor <b>1</b> (comparison of F <sup>-</sup> ion efflux efficiency at 450 sec) (B). Calculation of the initial rate of valinomycin-coupled F <sup>-</sup> ion efflux efficiency at different concentrations of receptor <b>1</b> (C and D). Concentration-dependent Cl <sup>-</sup> ion efflux studies of receptor <b>1</b> in the presence of valinomycin. LUVs were prepared in 10 mM HEPES buffer containing 300 mM KCl at pH 7.2 and suspended in 10 mM HEPES buffer containing 300 mM KGlc at pH 7.2 (E). Analysis of valinomycin-coupled Cl <sup>-</sup> ion efflux efficiency of receptor <b>1</b> (comparison of Cl <sup>-</sup> ion efflux efficiency at 450 sec) (F). Control experiment for temperature-dependent DPPC assay (G).	28
<b>Fig. S23.</b> Analysis of valinomycin-coupled F <sup>-</sup> and Cl <sup>-</sup> ion efflux efficiency of receptor <b>1</b> (comparison of Cl <sup>-</sup> ion efflux efficiency at 270 sec).	29
<b>References</b>	29

## Section S1. General information and instrumentation.

<sup>1</sup>H NMR spectra were recorded on 400 and 300 MHz Bruker NMR spectrometers using TMS as the internal standard. Chemical shifts are reported in parts per million (ppm). When peak multiplicities are given, the following abbreviations are used: s, singlet; br s, broad singlet; d, doublet; t, triplet; m, multiplet. <sup>13</sup>C NMR spectra were proton decoupled and recorded on a 100 MHz Bruker spectrometer using TMS as the internal standard. Isothermal titration calorimetry (ITC) titrations were performed at 298 K using a high-sensitive Standard Volume Nano ITC from TA instruments (Waters, New Castle, USA), and data acquisition was performed using manufacturer-supplied Nano Analyze software. Pyrrole was distilled at atmospheric pressure from CaH<sub>2</sub>. Titrations were performed using HPLC grade CH<sub>3</sub>CN. All other chemicals and solvents were purchased from commercial sources and were used as such unless otherwise mentioned.

## Section S2. Experimental section: synthetic scheme and synthetic procedures.



**Scheme S1.** Synthesis of receptors **1** and **2**.

### 2,2'-(1-(3,5-bis(trifluoromethyl)phenyl) ethane-1,1-diyl) bis(1H-pyrrole)4

To a solution of compound **3** (2.81 mL, 15.6 mmol) and pyrrole (20 mL, 288 mmol) was added TFA (3.6 mL, 46.8 mmol). The reaction mixture was stirred for 14h at room temperature and then diluted with water, followed by the addition of NaOH to neutralize the excess TFA. The organic part was extracted with  $\text{CHCl}_3$  (50 mL  $\times$  3). The combined organic layer was dried over anhydrous sodium sulfate. Evaporation of the organic layer under reduced pressure gave the crude product, which was then purified by column chromatography using 10% EtOAc in hexane as eluent to afford pure **4** as a white solid (Yield: 62%).  $^1\text{H}$  NMR (400 MHz,  $\text{CDCl}_3$ ):  $\delta$  7.84 (brs, 2H), 7.76 (s, 1H), 7.56 (s, 2H), 6.75-6.73 (m, 2H), 6.21-6.18 (m, 2H), 5.93-5.90 (m, 2H), 2.08 (s, 3H).  $^{13}\text{C}$  NMR (100 MHz,  $\text{CDCl}_3$ ):  $\delta$  150.5, 135.5, 131.4 (q,  $^2J_{\text{C-F}} = 33$  Hz), 127.7, 123.5 (q,  $^1J_{\text{C-F}} = 271$  Hz,  $\text{CF}_3$ ), 121.0, 118.2, 108.9, 107.3, 45.1, 28.8. HRMS  $m/z$  for  $\text{C}_{18}\text{H}_{15}\text{F}_6\text{N}_2$   $[\text{M}+\text{H}]^+$  calculated 373.1134, found 373.1134.

### Synthesis of calix[4]pyrrole **1** and **2**

Compound **3** (1 g, 2.68 mmol) was dissolved in 60mL acetone, and TFA (2.05 mL, 26.8 mmol) was added to the solution at 0°C under argon atmosphere. The reaction mixture was stirred for 5h and excess acetone distilled out, and 2M NaOH solution was added. The organic part was extracted with  $\text{CHCl}_3$  (50 mL  $\times$  3). The combined organic layer was dried over anhydrous sodium sulfate. Evaporation of the organic layer under reduced pressure gave the crude product, which was then purified by column chromatography using 5% EtOAc in hexane as eluent to afford pure **1** and **2** as white solid in 5% and 2% yields, respectively.

Receptor 1:  $^1\text{H}$  NMR (400 MHz,  $\text{CDCl}_3$ ):  $\delta$  7.73 (s, 2H), 7.4 (s, 4H), 7.25 (s, 4H), 5.96 (t,  $J = 4$  Hz, 4H), 5.59 (t,  $J = 4$  Hz, 4H), 1.94 (s, 6H), 1.64 (s, 6H), 1.52 (s, 6H).  $^{13}\text{C}$  NMR (100 MHz,  $\text{CDCl}_3$ ):  $\delta$  150.4, 139.3, 134.9, 130.9 (q,  $^2J_{\text{C-F}} = 34$  Hz), 127.6, 123.4 (q,  $^1J_{\text{C-F}} = 271$  Hz,  $\text{CF}_3$ ), 120.7, 106.6, 103.7, 44.8, 35.2, 29.9, 27.7, 27.4. HRMS  $m/z$  for  $\text{C}_{42}\text{H}_{37}\text{F}_{12}\text{N}_4$   $[\text{M}+\text{H}]^+$  calculated 825.2821, found 825.2821.

Receptor 2:  $^1\text{H}$  NMR (400 MHz,  $\text{CDCl}_3$ ):  $\delta$  7.75 (s, 2H), 7.52 (s, 4H), 7.22 (s, 4H), 5.96 (t,  $J = 4$  Hz, 4H), 5.72 (t,  $J = 4$  Hz, 4H), 1.93 (s, 6H), 1.53 (s, 12H).  $^{13}\text{C}$  NMR (100 MHz,  $\text{CDCl}_3$ ):  $\delta$  149.4, 139.6, 134.8, 131.1 (q,  $^2J_{\text{C-F}} = 33$  Hz), 127.6, 123.4 (q,  $^1J_{\text{C-F}} = 271$  Hz,  $\text{CF}_3$ ), 120.7, 106.6, 103.7, 44.9, 35.4, 29.1, 29.0. HRMS  $m/z$  for  $\text{C}_{42}\text{H}_{37}\text{F}_{12}\text{N}_4$   $[\text{M}+\text{H}]^+$  calculated 825.2821, found 825.2821.

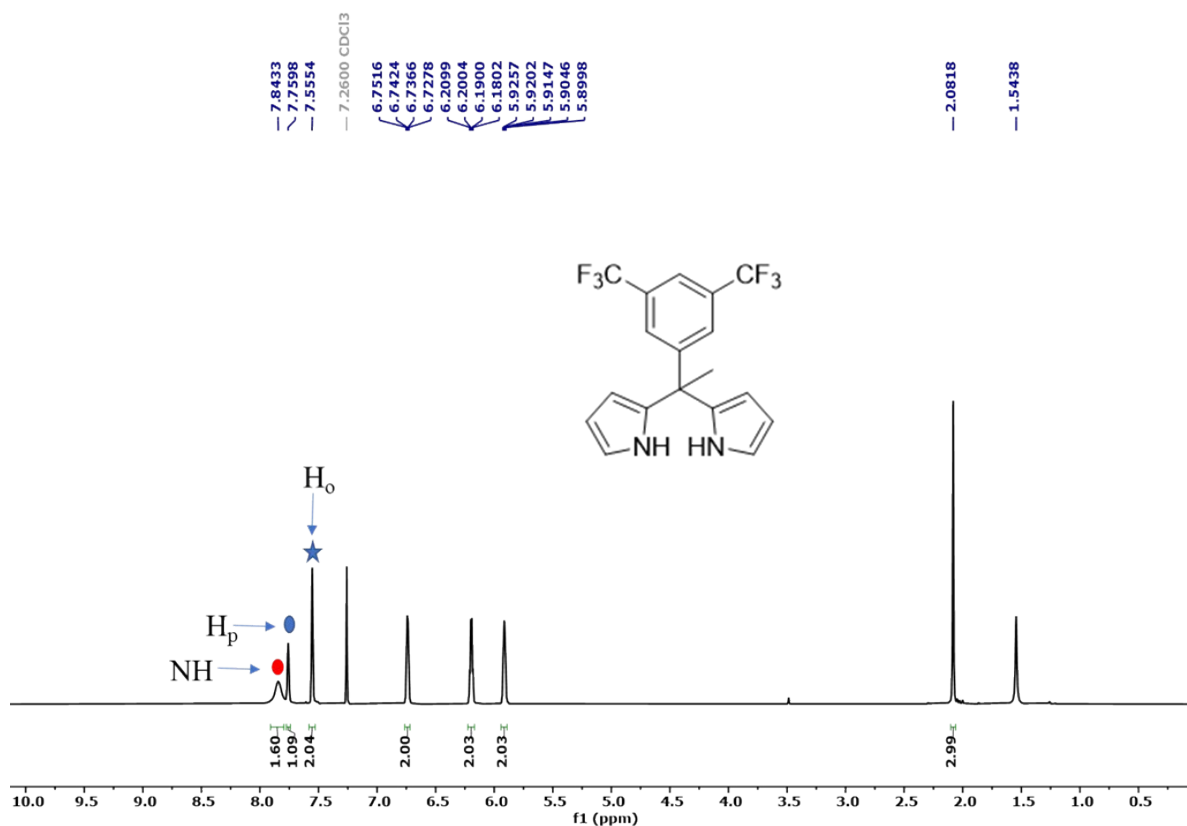


Fig. S1.  $^1\text{H}$  NMR spectrum of 4 in  $\text{CDCl}_3$ .

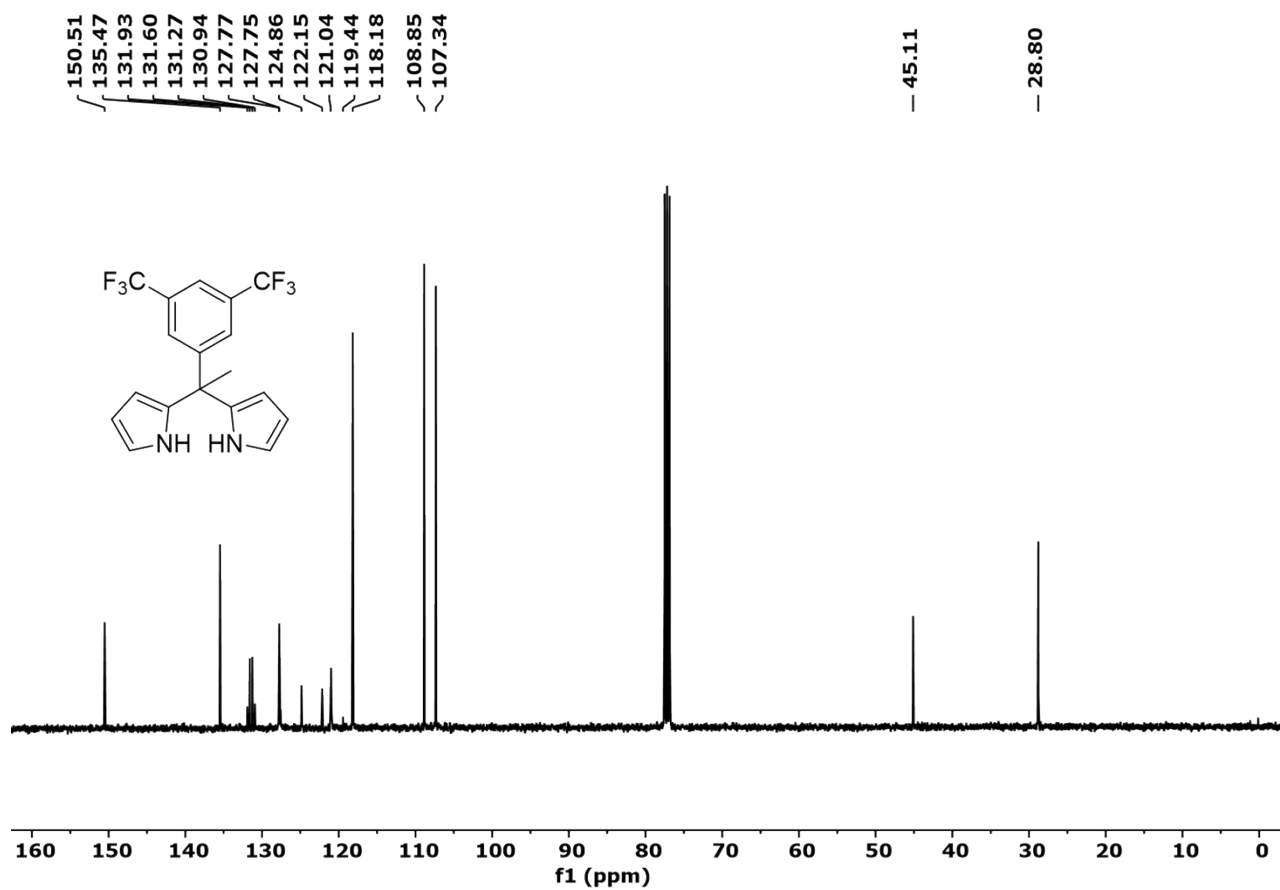


Fig. S2. <sup>13</sup>C NMR spectrum of 4 in CDCl<sub>3</sub>.

## Display Report

### Analysis Info

Analysis Name D:\Data\NEW USER DATA 2022\Jan-2022\25-jan-2022\Dr.D.Manna-DM-DP-41.d  
Method tune\_wide.m  
Sample Name DM-DP-41  
Comment

Acquisition Date 1/25/2022 2:46:21 PM  
Operator RUCHI  
Instrument micrOTOF-Q II 10330

### Acquisition Parameter

Source Type	ESI	Ion Polarity	Positive	Set Nebulizer	0.4 Bar
Focus	Not active	Set Capillary	4500 V	Set Dry Heater	180 °C
Scan Begin	50 m/z	Set End Plate Offset	-500 V	Set Dry Gas	4.0 l/min
Scan End	3000 m/z	Set Collision Cell RF	600.0 Vpp	Set Divert Valve	Source

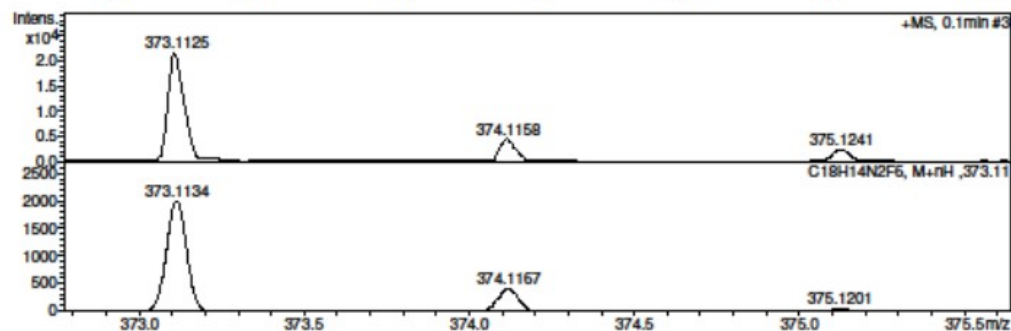
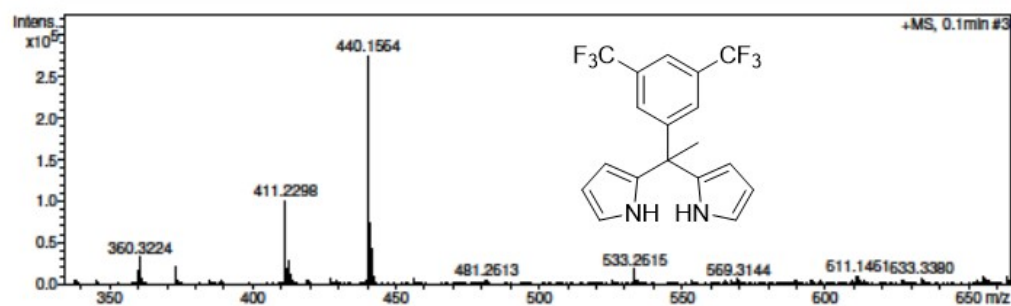
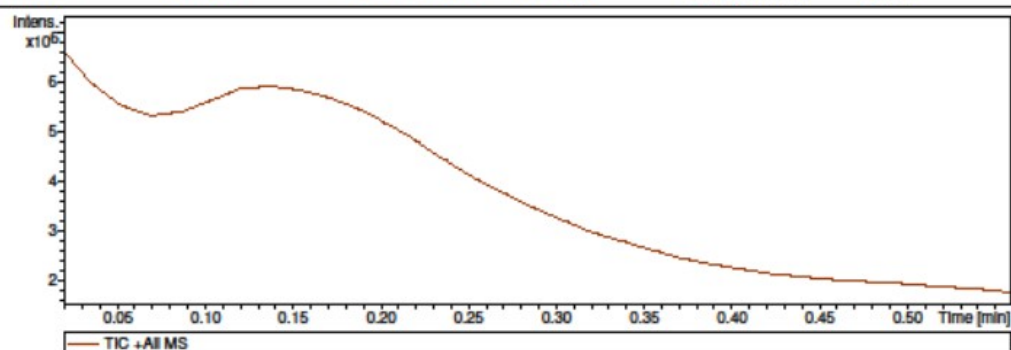
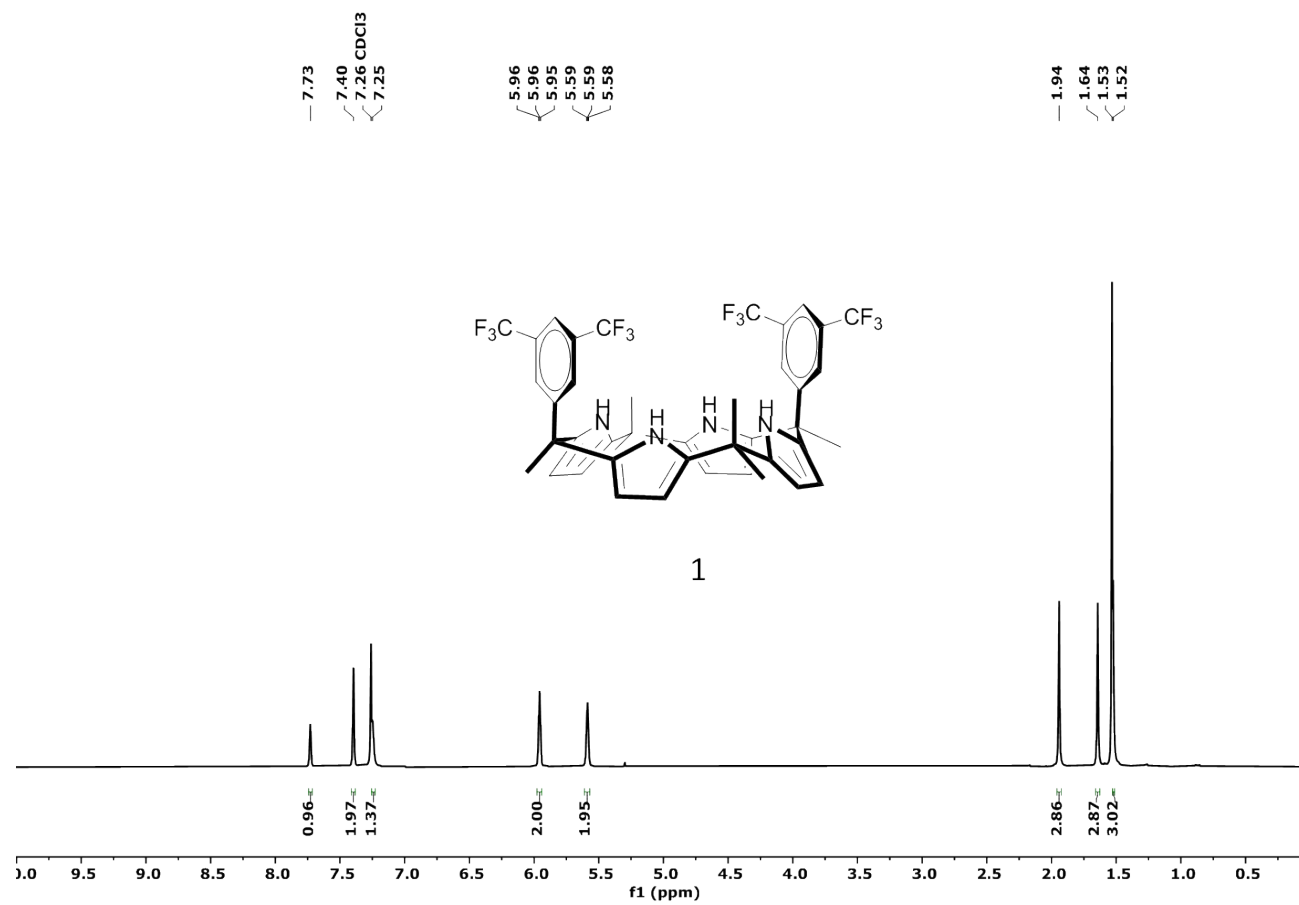


Fig. S3. HRMS spectrum of 4.



**Fig. S4.** <sup>1</sup>H NMR spectrum of **1** in CDCl<sub>3</sub>.

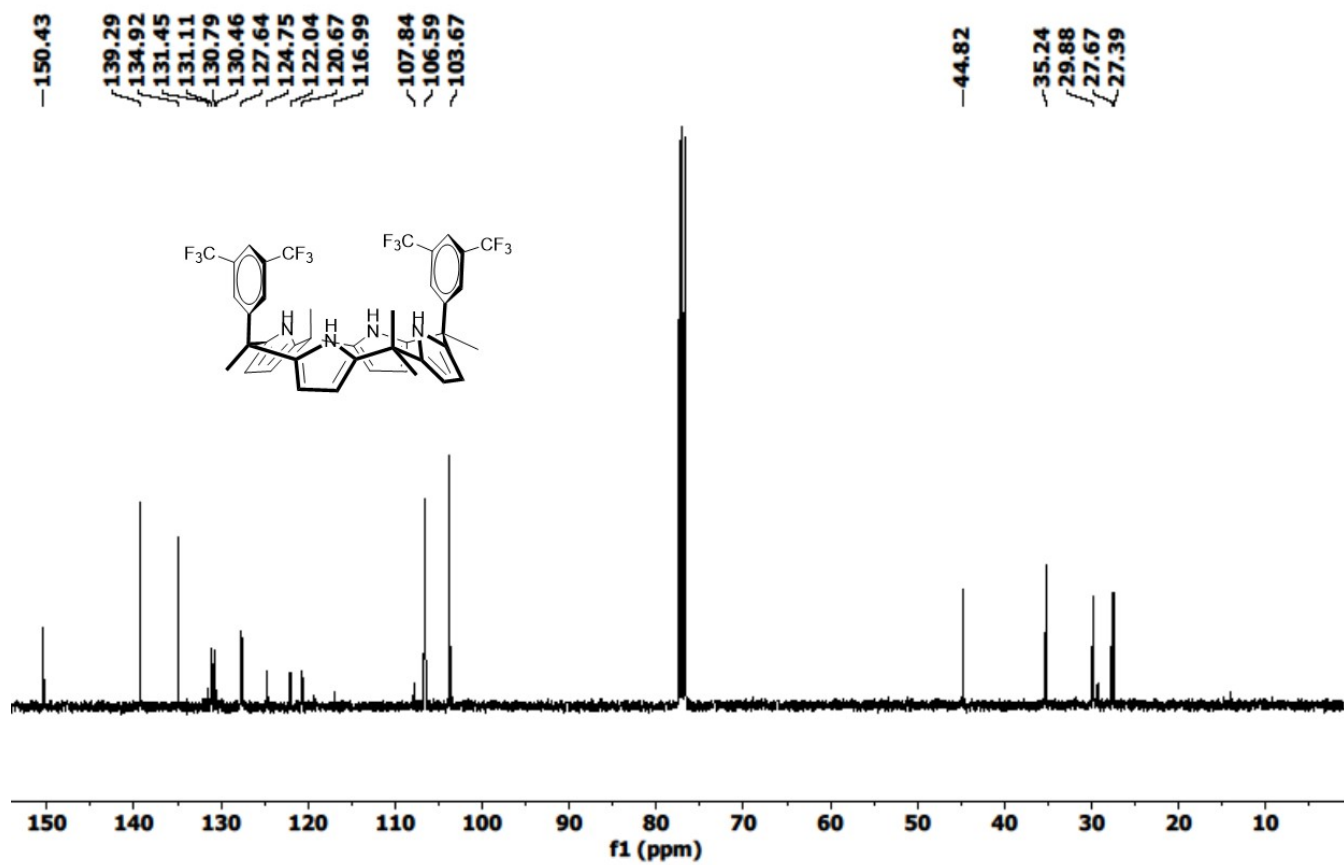


Fig. S5.  $^{13}\text{C}$  NMR spectrum of 1 in  $\text{CDCl}_3$ .



## Display Report

### Analysis Info

Analysis Name D:\Data\NEW USER DATA 2022\Jan-2022\25-jan-2022\Dr.D.Manna-DM-DP-43.d  
Method tune\_wide.m  
Sample Name DM-DP-43  
Comment

Acquisition Date 1/25/2022 2:50:41 PM

Operator RUCHI

Instrument micrOTOF-Q II 10330

### Acquisition Parameter

Source Type	ESI	Ion Polarity	Positive	Set Nebulizer	0.4 Bar
Focus	Not active	Set Capillary	4500 V	Set Dry Heater	180 °C
Scan Begin	50 m/z	Set End Plate Offset	-500 V	Set Dry Gas	4.0 l/min
Scan End	3000 m/z	Set Collision Cell RF	600.0 Vpp	Set Divert Valve	Source

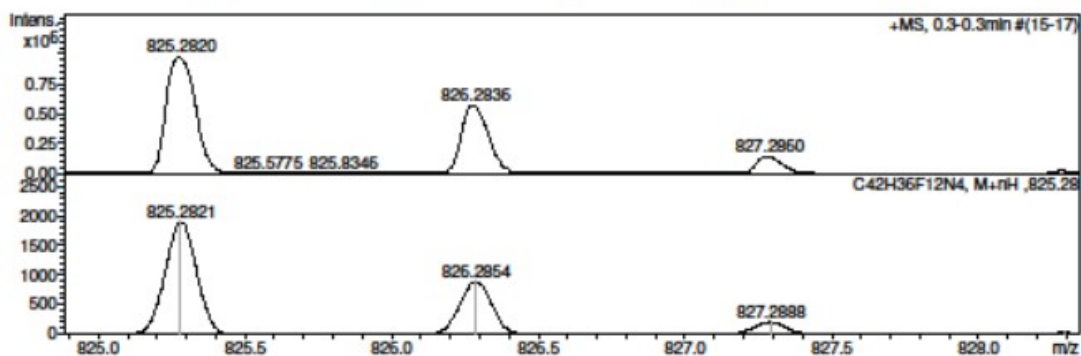
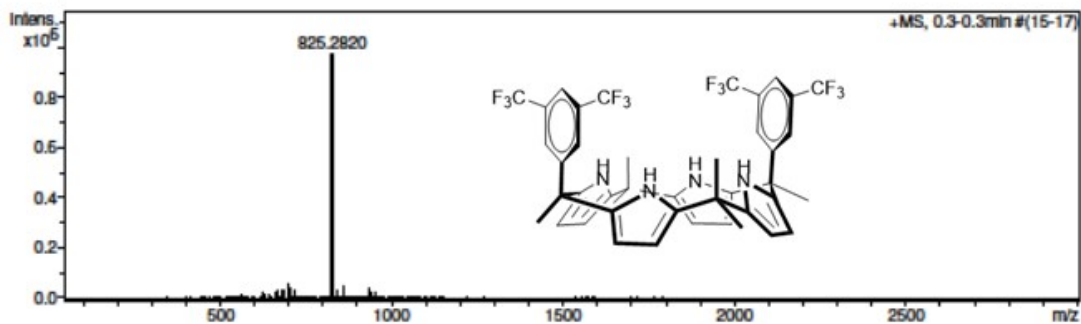
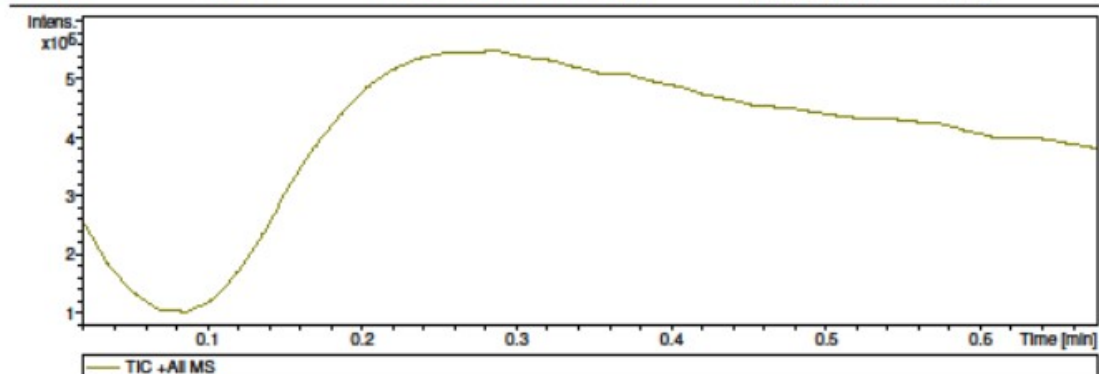


Fig. S6. HRMS spectrum of 1.

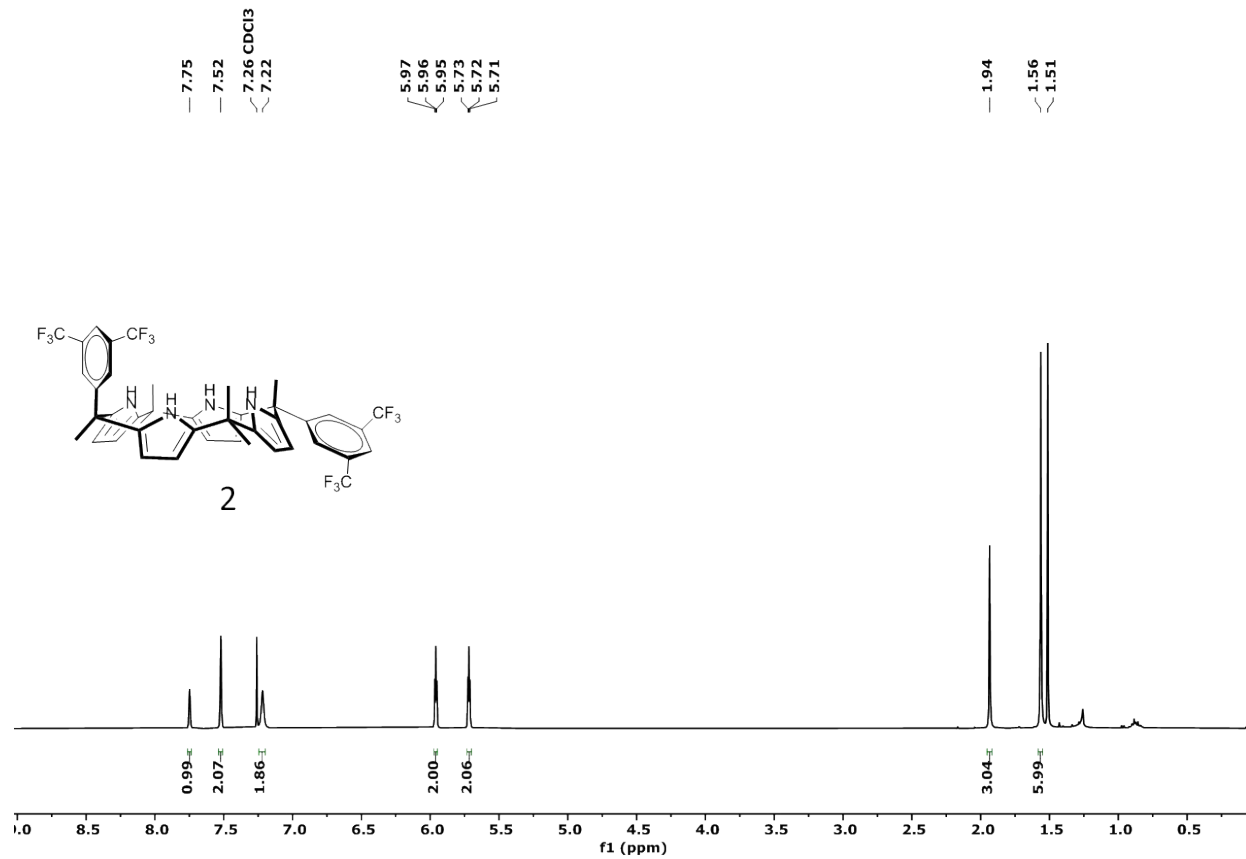


Fig. S7. <sup>1</sup>H NMR spectrum of **2** in CDCl<sub>3</sub>.

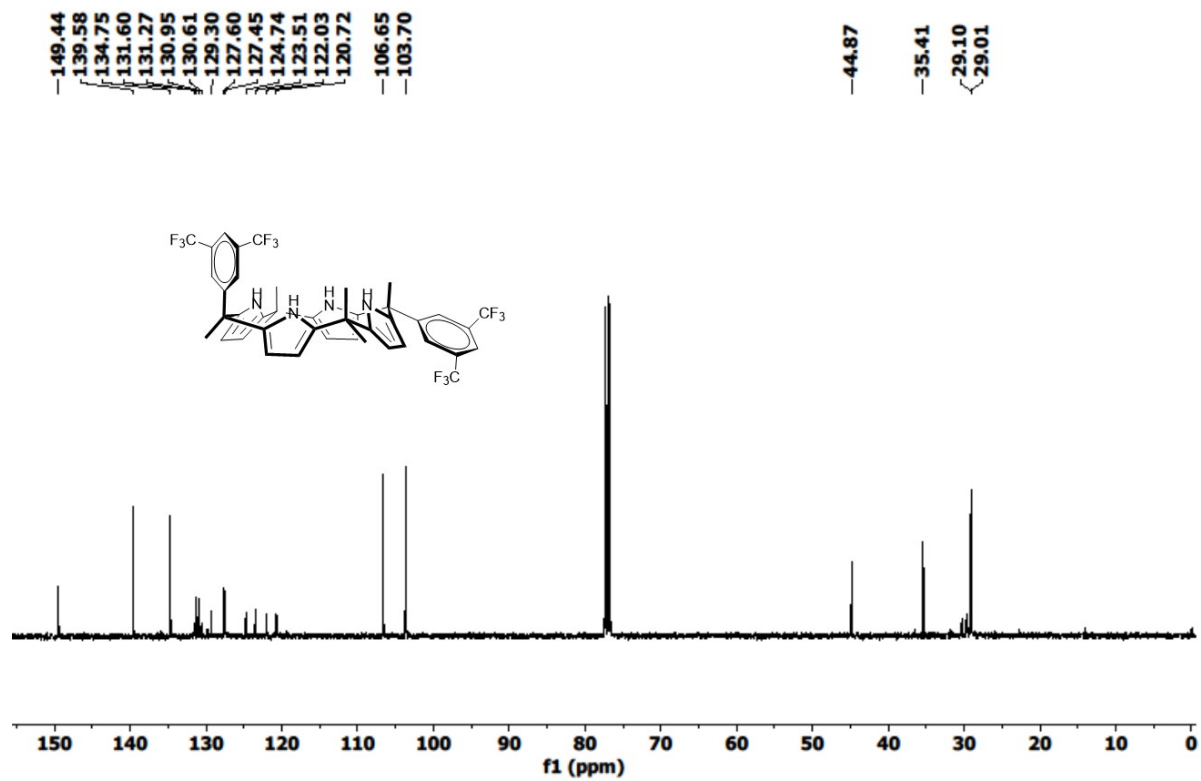


Fig. S8. <sup>13</sup>C NMR spectrum of 2 in CDCl<sub>3</sub>.

## Display Report

**Analysis Info**  
Analysis Name: D:\Data\NEW USER DATA 2022\Jan-2022\25-jan-2022\Dr.D.Manna-DM-DP-44.d  
Method: tune\_wide.m  
Sample Name: DM-DP-44  
Comment:  
Acquisition Date: 1/25/2022 2:52:20 PM  
Operator: RUCHI  
Instrument: micrOTOF-Q II 10330

**Acquisition Parameter**

Source Type	ESI	Ion Polarity	Positive	Set Nebulizer	0.4 Bar
Focus	Not active	Set Capillary	4500 V	Set Dry Heater	180 °C
Scan Begin	50 m/z	Set End Plate Offset	-500 V	Set Dry Gas	4.0 l/min
Scan End	3000 m/z	Set Collision Cell RF	600.0 Vpp	Set Divert Valve	Source

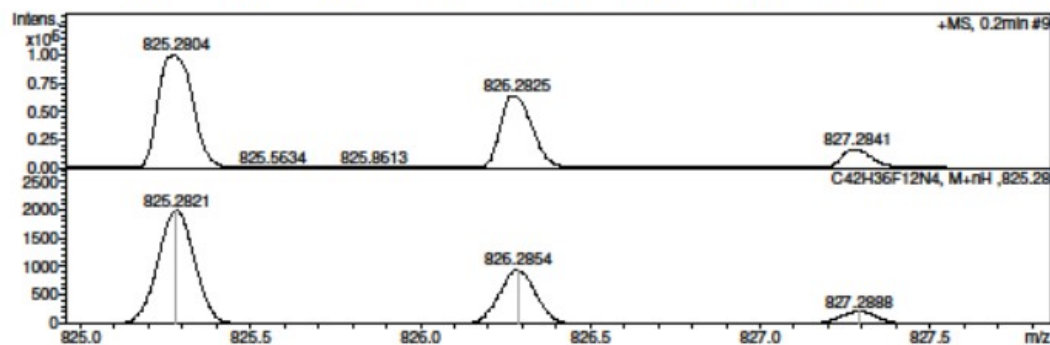
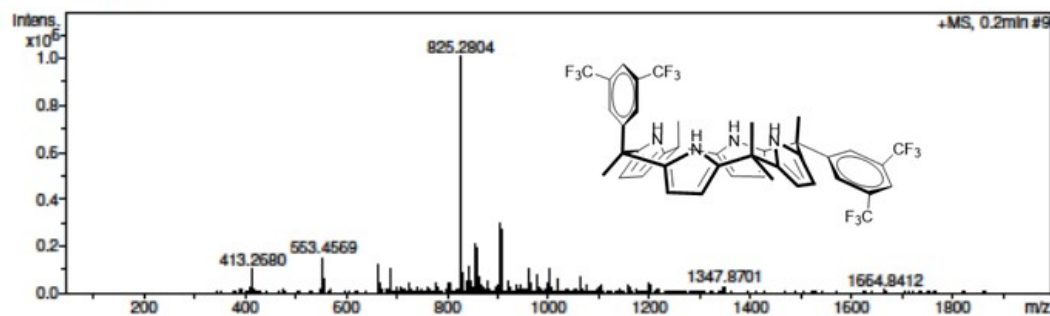
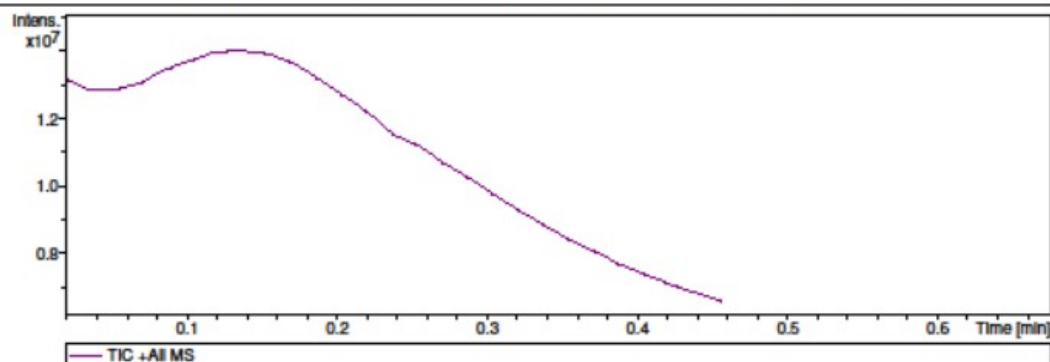
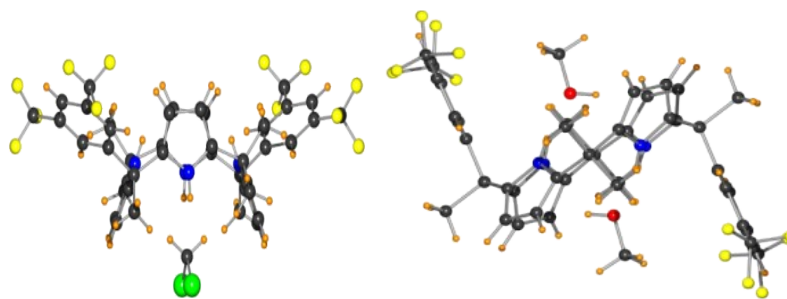
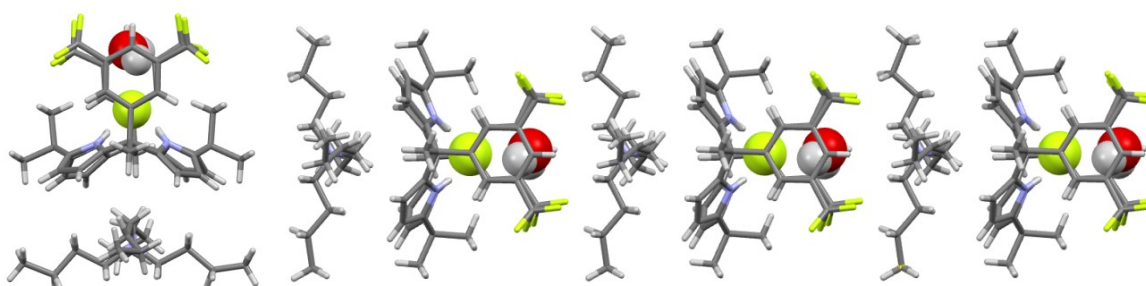


Fig. S9. HRMS spectrum of 2.



**Fig. S10.** Single crystal X-ray structures of **1**•CH<sub>2</sub>Cl<sub>2</sub> (left) and **2**•(CH<sub>3</sub>OH)<sub>2</sub> (right).



**Fig. S11.** Single crystal X-ray structure of **1**•TBAF•H<sub>2</sub>O complex (left) and partial view of the 1D linear supramolecular chain seen in the crystal lattice (right).

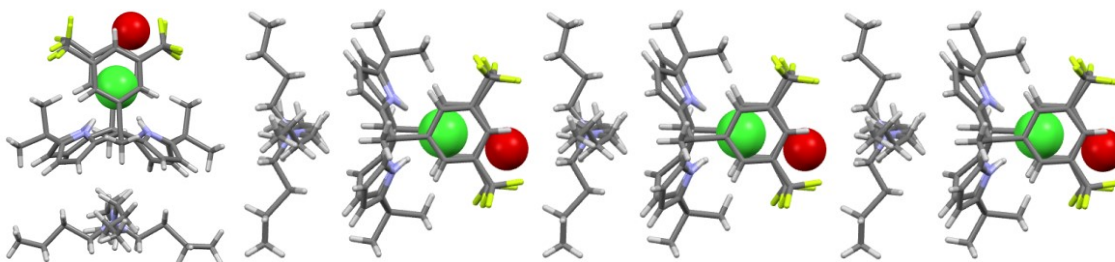


**Fig. S12.** Single crystal X-ray structure of **1**•TBACl•H<sub>2</sub>O complex (left) and partial view of the 1D linear supramolecular chain seen in the crystal lattice (right). H atoms of water could not be positioned reliably.

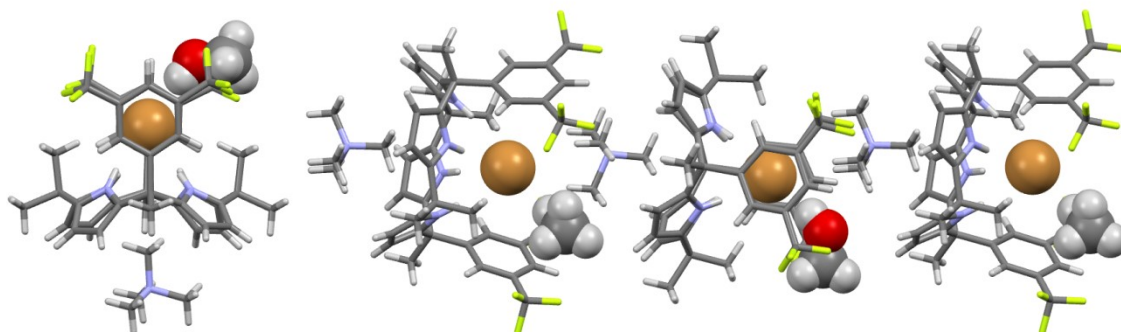


**Fig. S13.** Single crystal X-ray structure of **1**•TMABr•CH<sub>3</sub>OH complex (left) and partial view of the 1D linear supramolecular chain seen in the crystal lattice (right).

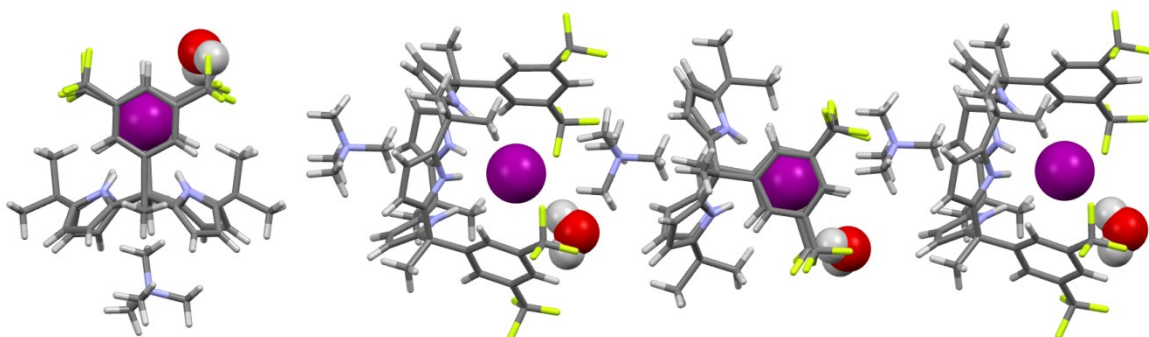


**Fig. S14.** Single crystal X-ray structure of **1**•TBAI•H<sub>2</sub>O complex (left) and partial view of the 1D linear supramolecular chain seen in the crystal lattice (right).

**Table S1.** Selected distances in the single crystal X-ray structures of fluoride, chloride, bromide and iodide complexes of **1**.

Complexes	N-H---A distances (Å)	N---A <sup>-</sup> distances (Å)	C-H---A <sup>-</sup> distances (Å)	<N-H---A <sup>-</sup> angle	Shortest distances between A <sup>-</sup> ---- centroids of phenyl ring (Å)	Distance between two centroids of phenyl rings (Å)	Distance between centroids of four N atoms of pyrrole and bound halide (Å)	Distances between centroids of pyrrole ring and N <sup>+</sup> atom of tetraalkylammonium cation (Å)	Anion---O distance between anion and bound H <sub>2</sub> O or CH <sub>3</sub> OH (Å)
<b>1</b> •TBAF•H <sub>2</sub> O	1.914, 1.923, 1.910, 1.943	2.764, 2.782, 2.770, 2.780	2.803, 2.825	169.27 163.91, 175.67, 178.32	3.954	7.391	1.555	5.107 5.032 4.983 4.860	2.690
<b>1</b> •TBACl•H <sub>2</sub> O	2.409, 2.408, 2.433, 2.399	3.275, 3.268, 3.256, 3.260	2.923, 2.961	173.84, 170.43, 177.18, 166.71	3.762	7.406	2.290	4.815, 4.941, 4.983, 5.098	3.013
<b>1</b> •TMABr•CH <sub>3</sub> OH	2.630, 2.604, 2.609, 2.633	3.490, 3.487, 3.456, 3.456	2.981, 2.952	174.83, 168.15, 173.95, 170.97	4.023	8.030	2.529	4.247 4.410, 4.501, 4.511	3.388
<b>1</b> •TMAI•H <sub>2</sub> O	2.792 2.828 2.806 2.849	3.665, 3.726, 3.703, 3.682	3.002, 3.140	172.50 173.34 173.68 171.25	4.032	8.073	2.806	4.218, 4.435, 4.499, 4.511	3.694

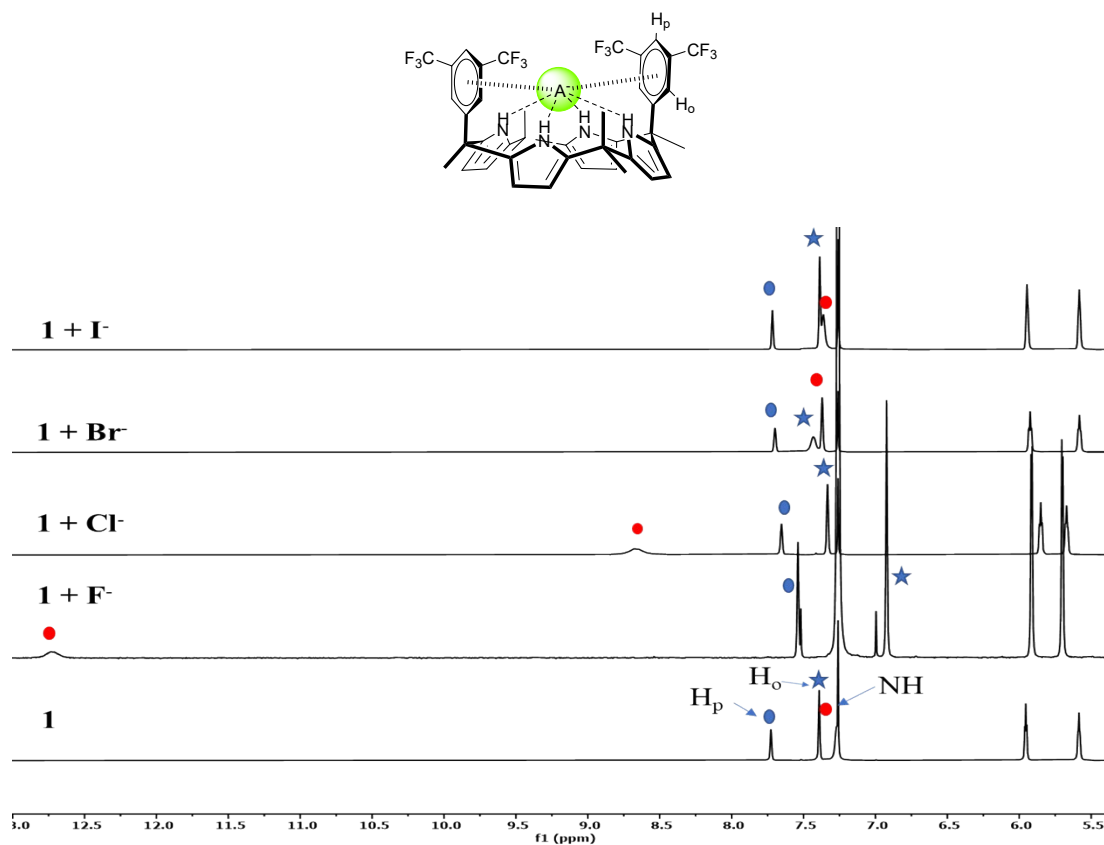


**Fig. S15.** Partial  $^1\text{H}$ NMR spectra of **1** recorded in the presence and absence of ca. 5.0 equivalent amounts of TBAX ( $X = \text{F}^-$ ,  $\text{Cl}^-$ ,  $\text{Br}^-$  and  $\text{I}^-$ ) in  $\text{CDCl}_3$ .



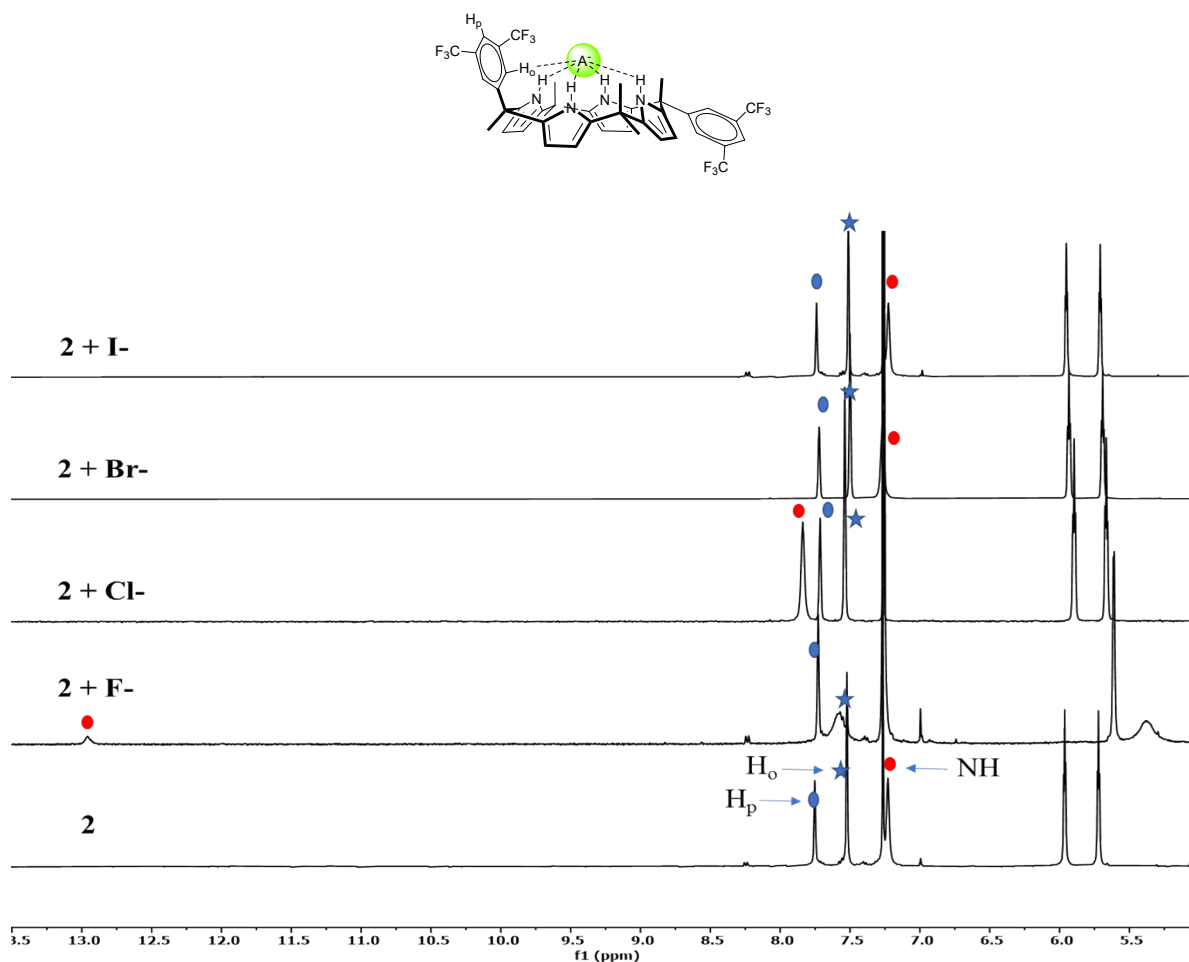


**Fig. S16.** Partial  $^1\text{H}$ NMR spectra of **2** recorded in the presence and absence of ca. 5.0 equivalent amounts of TBAX ( $X = \text{F}^-$ ,  $\text{Cl}^-$ ,  $\text{Br}^-$  and  $\text{I}^-$ ) in  $\text{CDCl}_3$ .

**Table S2.** Association constant values ( $K_a$  in  $\text{M}^{-1}$ ) and thermodynamic parameters for the interaction of receptors **1** and **2** with fluoride and chloride anions (as their tetrabutylammonium salts) in  $\text{CH}_3\text{CN}$  measured by isothermal titration calorimetry at 298 K.

Receptors	anions	$K_a$ in $\text{M}^{-1}$	$\Delta G$ in kcal/mol	$\Delta H$ in kcal/mol	$T\Delta S$ in kcal/mol
<b>1</b>	Fluoride	$1.34 \times 10^6$	-8.36	-4.02	4.34
	Chloride	$6.14 \times 10^5$	-7.896	-6.749	1.147
<b>2</b>	Fluoride	$1.16 \times 10^6$	-8.271	-3.476	4.795
	Chloride	$1.23 \times 10^4$	-5.581	-3.976	1.605

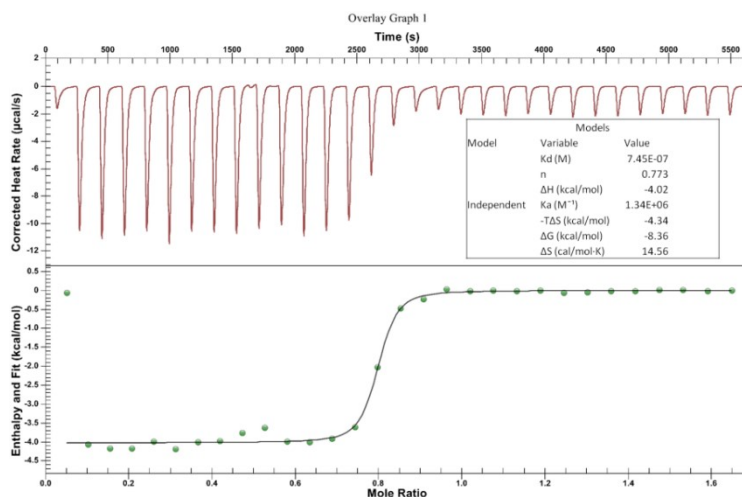


**Fig. S17.** ITC plots showing titrations of receptor **1** (initial concentrations: 1.39 mM) with TBAF (17.03 mM) in CH<sub>3</sub>CN at 298 K.

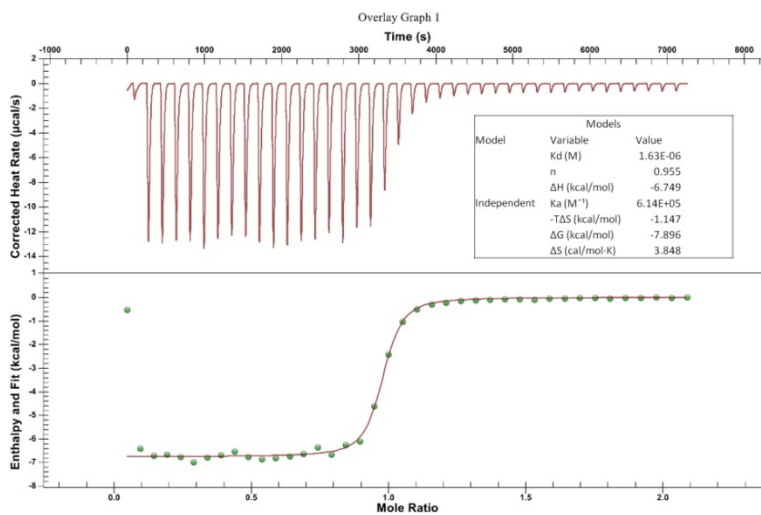


**Fig. S18.** ITC plots showing titrations of receptor **1** (initial concentrations: 1.33 mM) with TBACl (15.11 mM) in CH<sub>3</sub>CN at 298 K.

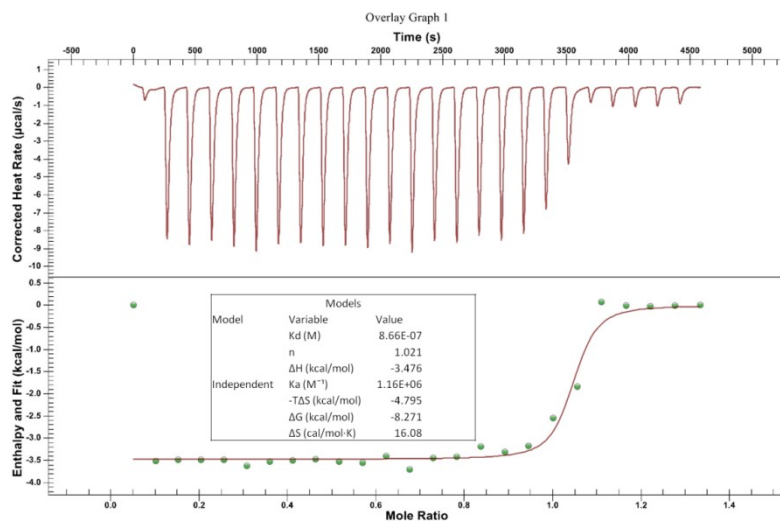


**Fig. S19.** ITC plots showing titrations of receptor **2** (initial concentrations: 1.45mM) with TBAF (17.43 mM) in CH<sub>3</sub>CN at 298 K.

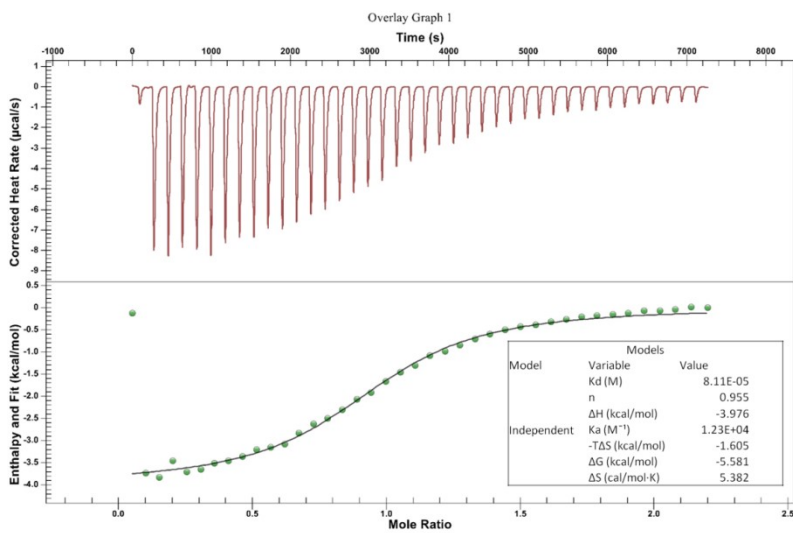


**Fig. S20.** ITC plots showing titrations of receptor **2** (initial concentrations: 1.45 mM) with TBACl (17.39 mM) in CH<sub>3</sub>CN at 298 K.

### Section S3. Experimental details for single crystal X-ray structure determination

Suitable single crystals of all organic compounds were mounted on a Bruker AXS D8 QUEST ECO (Mo) diffractometer equipped with a graphite monochromator and Mo-K $\alpha$  ( $\lambda = 0.71073 \text{ \AA}$ ) radiation. Unit cell parameters were determined by using the APEX2<sup>1</sup> program. Data reduction was carried out by the SAINT<sup>1</sup> program, and correction or absorption was performed using the SADABS<sup>1</sup> program. The structure was solved using the Patterson method by using the SHELXS-2018/3<sup>2</sup> embedded in WINGX software package<sup>3</sup> and refined using SHELXL-2018/3.<sup>4</sup> Subsequent difference Fourier synthesis and least-square refinement revealed the positions of the remaining non-hydrogen atoms. Non-hydrogen atoms were refined with independent anisotropic displacement parameters. All other hydrogen atoms were placed in idealized positions and their displacement parameters were fixed to be 1.2 times larger than those of the attached non-hydrogen atom. All Fig.s were drawn by using PLATON<sup>5</sup> and ORTEP<sup>6</sup>. Data collection and structure refinement parameters and crystallographic data for all the compounds are given in Table S3-S5.

#### 1. X-ray experimental for complex of **1** with tetrabutylammonium fluoride

Single crystals of **1**•TBA<sup>+</sup>•F<sup>-</sup>•H<sub>2</sub>O were obtained as colorless needles via the slow evaporation of a CHCl<sub>3</sub>/CH<sub>3</sub>OH (4:1, v/v) solution of receptor **1** in the presence of tetrabutylammonium fluoride. Several fluorine atoms present in the -CF<sub>3</sub> groups are in disordered position, and the structure was refined following the disorder model.

#### 2. X-ray experimental for complex of **1** with tetrabutylammonium chloride

Single crystals of **1**•TBA<sup>+</sup>•Cl<sup>-</sup>•H<sub>2</sub>O were obtained as colorless needles via the slow evaporation of a CHCl<sub>3</sub>/CH<sub>3</sub>OH (4:1, v/v) solution of receptor **1** in the presence of tetrabutylammonium chloride. Several fluorine atoms present in the -CF<sub>3</sub> groups are in disordered position and the structure was refined following the disorder model. Due to the disorderliness of the guest water molecule, the hydrogen atoms can't be located.

#### 3. X-ray experimental for complex of **1** with tetramethylammonium bromide

Single crystals of **1**•TMA<sup>+</sup>•Br<sup>-</sup>•CH<sub>3</sub>OH were obtained as colorless needles via the slow evaporation of a CHCl<sub>3</sub>/CH<sub>3</sub>OH (4:1, v/v) solution of receptor **1** in the presence of tetramethylammonium bromide.

#### 4. X-ray experimental for complex of **1** with tetramethylammonium iodide

Single crystals of **1**•TMA<sup>+</sup>•I<sup>-</sup>•H<sub>2</sub>O were obtained as colorless needles via the slow evaporation of a CHCl<sub>3</sub>/CH<sub>3</sub>OH (4:1, v/v) solution of receptor **1** in the presence of tetramethylammonium iodide. Several fluorine atoms present in the -CF<sub>3</sub> groups are disordered, and the structure was refined following the disorder model.

#### 5. X-ray experimental for free host **1**•DCM

Single crystals of receptor **1** were obtained as colorless needles via the slow evaporation of DCM solution of receptor **1**.

## 6. X-ray experimental for free host $2 \cdot (\text{CH}_3\text{OH})_2$

Single crystals of  $2 \cdot \text{CH}_3\text{OH}$  were obtained as colorless needles via the slow evaporation of the  $\text{CH}_3\text{OH}$  solution of receptor **2**. Several fluorine atoms present in the  $-\text{CF}_3$  groups are disordered, and the structure was refined following the disorder model.

**Table S3.** Selected crystal data and refinement parameters for receptor  $1 \cdot \text{CH}_2\text{Cl}_2$  and  $2 \cdot (\text{CH}_3\text{OH})_2$ .

Identification code	$1 \cdot \text{CH}_2\text{Cl}_2$	$2 \cdot (\text{CH}_3\text{OH})_2$
Empirical formula	$\text{C}_{43}\text{H}_{38}\text{N}_4\text{F}_{12}\text{Cl}_2$	$\text{C}_{44}\text{H}_{44}\text{N}_4\text{F}_{12}\text{O}_2$
Formula weight	909.67	888.83
Temperature/K	273(2)	273(2)
Crystal system	orthorhombic	monoclinic
Space group	$\text{P}2_12_12$	$\text{C}2/\text{c}$
$a/\text{\AA}$	19.6810(7)	25.1735(8)
$b/\text{\AA}$	10.2423(4)	9.9028(3)
$c/\text{\AA}$	10.6706(4)	18.7477(6)
$\alpha/^\circ$	90	90
$\beta/^\circ$	90	104.647(2)
$\gamma/^\circ$	90	90
Volume/ $\text{\AA}^3$	2150.97(14)	4521.7(2)
$Z$	2	4
$\rho_{\text{calc}}/\text{g/cm}^3$	1.405	1.306
$\mu/\text{mm}^{-1}$	0.239	0.115
$F(000)$	932.0	1840.0
Crystal size/ $\text{mm}^3$	$0.12 \times 0.1 \times 0.08$	$0.12 \times 0.1 \times 0.08$
Radiation	$\text{MoK}\alpha$ ( $\lambda = 0.71073$ )	$\text{MoK}\alpha$ ( $\lambda = 0.71073$ )
$2\Theta$ range for data collection/ $^\circ$	4.342 to 41.66	4.44 to 42.482
Index ranges	$-19 \leq h \leq 19, -10 \leq k \leq 10, -10 \leq l \leq 10$	$-25 \leq h \leq 25, -10 \leq k \leq 10, -19 \leq l \leq 19$
Reflections collected	22893	26435
Independent reflections	2260 [ $R_{\text{int}} = 0.0910, R_{\text{sigma}} = 0.0456$ ]	2502 [ $R_{\text{int}} = 0.0444, R_{\text{sigma}} = 0.0215$ ]
Data/restraints/parameters	2260/0/277	2502/0/348
Goodness-of-fit on $F^2$	1.056	1.075
Final R indexes [ $I \geq 2\sigma(I)$ ]	$R_1 = 0.0732, wR_2 = 0.1876$	$R_1 = 0.0433, wR_2 = 0.1163$
Final R indexes [all data]	$R_1 = 0.0889, wR_2 = 0.1993$	$R_1 = 0.0520, wR_2 = 0.1213$
Largest diff. peak/hole / $e \text{\AA}^{-3}$	0.47/-0.34	0.22/-0.17
Flack parameter	-0.2(6)	
<b>CCDC number</b>	<b>CCDC 2237711</b>	<b>CCDC 2237712</b>

**Table S4.** Selected crystal data and refinement parameters for **1•TBAF•H<sub>2</sub>O** and **1•TBACl•H<sub>2</sub>O**.

Identification code	<b>1•TBAF•H<sub>2</sub>O</b>	<b>1•TBACl•H<sub>2</sub>O</b>
Empirical formula	C <sub>58</sub> H <sub>74</sub> F <sub>12</sub> N <sub>5</sub> O	C <sub>58</sub> H <sub>74</sub> ClN <sub>5</sub> F <sub>12</sub> O
Formula weight	1085.22	1120.67
Temperature/K	299(2)	273(2)
Crystal system	orthorhombic	orthorhombic
Space group	Pna2 <sub>1</sub>	Pna2 <sub>1</sub>
a/Å	21.8214(16)	21.6302(8)
b/Å	13.2329(10)	13.5934(5)
c/Å	20.7744(16)	20.6884(7)
α/°	90	90
β/°	90	90
γ/°	90	90
Volume/Å <sup>3</sup>	5998.8(8)	6083.0(4)
Z	4	4
ρ <sub>calc</sub> /g/cm <sup>3</sup>	1.202	1.224
μ/mm <sup>-1</sup>	0.097	0.141
F(000)	2292.0	2360.0
Crystal size/mm <sup>3</sup>	0.16 × 0.12 × 0.08	0.16 × 0.12 × 0.08
Radiation	MoKα (λ = 0.71073)	MoKα (λ = 0.71073)
2θ range for data collection/°	3.6 to 52.752	4.05 to 54.942
Index ranges	-27 ≤ h ≤ 23, -16 ≤ k ≤ 16, -17 ≤ l ≤ 25	-27 ≤ h ≤ 27, -17 ≤ k ≤ 17, -26 ≤ l ≤ 26
Reflections collected	28242	114431
Independent reflections	10159 [R <sub>int</sub> = 0.0533, R <sub>sigma</sub> = 0.0715]	13874 [R <sub>int</sub> = 0.1766, R <sub>sigma</sub> = 0.1174]
Data/restraints/parameters	10159/32/767	13874/9/699
Goodness-of-fit on F <sup>2</sup>	1.021	0.997
Final R indexes [I ≥ 2σ (I)]	R <sub>1</sub> = 0.0730, wR <sub>2</sub> = 0.1920	R <sub>1</sub> = 0.0957, wR <sub>2</sub> = 0.2255
Final R indexes [all data]	R <sub>1</sub> = 0.1566, wR <sub>2</sub> = 0.2574	R <sub>1</sub> = 0.2095, wR <sub>2</sub> = 0.2847
Largest diff. peak/hole / e Å <sup>-3</sup>	0.35/-0.24	0.47/-0.29
Flack parameter	2.0(15)	0.25(17)
<b>CCDC number</b>	<b>CCDC 2237713</b>	<b>CCDC 2237714</b>

**Table S5.** Selected crystal data and refinement parameters for **1•TMABr•CH<sub>3</sub>OH** and **1•TMAI•H<sub>2</sub>O**.

Identification code	<b>1•TMABr•CH<sub>3</sub>OH</b>	<b>1•TMAI•H<sub>2</sub>O</b>
Empirical formula	C <sub>47</sub> H <sub>52</sub> N <sub>5</sub> OBrF <sub>12</sub>	C <sub>91</sub> H <sub>100</sub> F <sub>24</sub> I <sub>2</sub> N <sub>10</sub> O <sub>2</sub>
Formula weight	1010.84	2075.60
Temperature/K	273(2)	164(2)
Crystal system	monoclinic	monoclinic
Space group	P2 <sub>1</sub> /c	P2 <sub>1</sub> /c
a/Å	11.1101(15)	11.118(7)
b/Å	20.791(3)	20.761(14)
c/Å	21.126(3)	21.874(14)
α/°	90	90
β/°	101.012(2)	102.455(8)
γ/°	90	90
Volume/Å <sup>3</sup>	4790.0(11)	4930(6)
Z	4	2
ρ <sub>calc</sub> /g/cm <sup>3</sup>	1.402	1.398
μ/mm <sup>-1</sup>	0.945	0.733
F(000)	2080.0	2108.0
Crystal size/mm <sup>3</sup>	0.16 × 0.12 × 0.08	0.12 × 0.1 × 0.08
Radiation	MoKα (λ = 0.71073)	MoKα (λ = 0.71073)
2θ range for data collection/°	4.876 to 38.056	4.738 to 53.09
Index ranges	-10 ≤ h ≤ 10, -19 ≤ k ≤ 19, -19 ≤ l ≤ 19	-13 ≤ h ≤ 13, -25 ≤ k ≤ 25, -27 ≤ l ≤ 27
Reflections collected	26732	59123
Independent reflections	3837 [R <sub>int</sub> = 0.0599, R <sub>sigma</sub> = 0.0352]	10097 [R <sub>int</sub> = 0.5509, R <sub>sigma</sub> = 0.4249]
Data/restraints/parameters	3837/0/596	10097/36/588
Goodness-of-fit on F <sup>2</sup>	1.163	0.982
Final R indexes [I >= 2σ (I)]	R <sub>1</sub> = 0.0899, wR <sub>2</sub> = 0.2291	R <sub>1</sub> = 0.1420, wR <sub>2</sub> = 0.2870
Final R indexes [all data]	R <sub>1</sub> = 0.0972, wR <sub>2</sub> = 0.2365	R <sub>1</sub> = 0.3536, wR <sub>2</sub> = 0.3819
Largest diff. peak/hole / e Å <sup>-3</sup>	1.50/-0.75	1.26/-1.60
<b>CCDC number</b>	<b>CCDC 2237715</b>	<b>CCDC 2237716</b>

#### Section S4. Experimental details of anion transport studies

**EYPC/Chol vesicle preparation** — The transmembrane ion transport studies were performed using the large unilamellar vesicles (LUVs) compound of egg yolk phosphatidylcholine (EYPC), and cholesterol (Chol) encapsulated with fluoride or chloride salts. The LUVs were prepared by following a previously established method.<sup>7,8</sup> Briefly, a thin lipid film was prepared using EYPC

(stock concentration: 50 mg/mL in deacidified  $\text{CHCl}_3$ ) and Chol (stock concentration: 25 mg/mL in deacidified  $\text{CHCl}_3$ ), taken in a clean glass vial in the molar ratio of 8:2. The lipid solution was dried under reduced pressure for 6 h and then hydrated with 10 mM HEPES buffer containing 300 mM KF at pH 7.2 or 10 mM HEPES buffer containing 300 mM KCl at pH 7.2 buffer (800  $\mu\text{L}$ ) for 40 minutes with continuous vortexing. The cloudy suspension was then subjected to 11 freeze-thaw cycles (freezing with liquid nitrogen and melting at 70 °C, respectively) to break up the multilamellar vesicles, if any formed. The resulting solution was then vortexed for 10 mins and extruded through a polycarbonate membrane (pore size: 200 nm, Avanti polar lipids) using a mini extruder 19-21 times. To remove any unencapsulated components, LUVs were dialyzed overnight with 10 mM HEPES buffer containing 300 mM KGlc at pH 7.2. Fractions of dialyzed liposome were collected, and volume was made up to 500  $\mu\text{L}$  with 10 mM HEPES buffer containing 300 mM KGlc at pH 7.2.

**DPPC vesicle preparation**— The DPPC containing LUVs was prepared in 10 mM HEPES buffer containing 300 mM KF at pH 7.2. The vesicles were prepared following a previously given method.<sup>7,8</sup> A thin film of the lipid was prepared by evaporation of 50  $\mu\text{L}$  solution of DPPC (stock concentration: 100 mg/mL in deacidified  $\text{CHCl}_3$ ). This film was dried under reduced pressure for 6 h. A buffered KF solution (500  $\mu\text{L}$ , 10 mM HEPES buffer containing 300 mM KF at pH 7.2) was then added at 47 °C, resulting in a suspension which was then subjected to 13 freeze-thaw cycles (liquid nitrogen, 70 °C water bath), sonicated for 30 mins (with occasional incubation in ice water medium) and extruded 19-21 times through a 200 nm polycarbonate membrane (Avanti polar lipids) at 47 °C. Fractions of dialyzed liposome were collected, and volume was made up to 500  $\mu\text{L}$  with 10 mM HEPES buffer containing 300 mM KGlc at pH 7.2. Vesicle concentration was calculated assuming full conversion of EYPC lipids into the vesicles within aqueous medium.

**Fluoride efflux in the absence of valinomycin**— The transport assay was adapted from a previous report.<sup>7</sup> The EYPC/Chol-LUVs prepared in 10 mM HEPES buffer containing 300 mM KF at pH 7.2 was suspended in 10 mM HEPES buffer containing 300 mM KGlc at pH 7.2 (4 mL). After the electrode voltage had stabilized (~30 s), the measurement was initiated using a fluoride-selective electrode (F-ISE). At  $t = 50$  s, DMSO and the active transporters (10  $\mu\text{L}$ ) were injected into the vesicle solution. At  $t = 450$  s, 20  $\mu\text{L}$  of a Triton X solution (20% Triton X-100 in



water (v/v)) was added to lyse the vesicles triggering the complete release of the F<sup>-</sup> ion. The value corresponding to 100% F<sup>-</sup> ion efflux was recorded at t = 700s, 12 min. After lysing the vesicles, it was found that in the absence of a cationophore (valinomycin), F<sup>-</sup> ion efflux was quite negligible.

**Fluoride efflux in the presence of valinomycin** — The transport assay was adapted from a previous report.<sup>7</sup> The EYPC/Chol-LUVs prepared in 10 mM HEPES buffer containing 300 mM KF at pH 7.2 were suspended in 10 mM HEPES buffer containing 300 mM KGlc at pH 7.2 (4 mL). After the electrode voltage had stabilized (~30 s), the measurement was initiated using a fluoride-selective electrode (F-ISE). At t = 0 s, valinomycin dissolved in DMSO (1 μM) was added. At t = 30s, the synthetic transporters (10 μL) were added to the assay. At t = 450s, 20 μL of a Triton X-100 solution (20% Triton X-100 in water (v/v)) was added to lyse the vesicles triggering the complete release of the F<sup>-</sup> ion. The value corresponding to 100% F<sup>-</sup> ion efflux was recorded at t = 700 s, 12 min after lysing the vesicles. The resulting data were fitted to the Hill equation to get the EC<sub>50</sub> concentration of the transporter.

**Hill plot measurements and analysis**—The binding affinity was calculated using Hill plot analysis according to the following equation:

$$y = V_{max} \frac{x^n}{k^n + x^n}$$

$x$  is the carrier concentration in μM. The  $V_{max}$ ,  $k$ , and  $n$  were the parameters to be fit.  $V_{max}$  is the maximum efflux possible (usually fixed to 100% as this is the maximum salt efflux possible),  $n$  is the Hill coefficient, and  $k$  is the carrier concentration needed to reach  $V_{max}/2$  (when  $V_{max}$  is fixed to 100%,  $k$  is EC<sub>50</sub>). The EC<sub>50</sub> values at 450 s can be obtained directly from the Hill plot.

**Initial rate of fluoride ion efflux** — The initial rate of F<sup>-</sup> ion efflux was calculated by using a non-linear curve fitting analysis (asymptotic function) of the concentration-dependent F<sup>-</sup> ion efflux measurements.<sup>7</sup>

$$y = a - b.c^x$$

$$y = \% \text{ F}^- \text{ ion efflux}$$

$$x = \text{time (s)}$$

$$k_{ini} = -b \cdot \ln(c) \text{ (\% s}^{-1}\text{)}$$

The resulting initial rate of  $F^-$  ion efflux was fitted to the Hill equation to get the  $EC_{50}'$  concentration of the transporter.

**Fluoride transport experiments across a  $CH_2Cl_2$  phase in a U-Tube experiment** — The U-tube was loaded with a  $CH_2Cl_2$  solution (8 mL) containing compound **1** as a transporter (3 mM) and  $TBAPF_6$  (6 mM) as an electrolyte.<sup>7,8</sup> The right arm of the U-tube was filled with deionized water (10 mL) containing KF solution. The left arm was filled with deionized water (10 mL). A magnetic bar placed at the bottom of the U-tube was used to stir the  $CH_2Cl_2$  solution vigorously. The fluoride ion concentration in the receiving water phase (left arm of the U-tube) was monitored by F-ISE and compared to that of a blank. This blank was prepared by using an identical U-tube, loaded with solutions of the same composition, except compound **1** was omitted from the  $CH_2Cl_2$  solution.

**Temperature-dependent fluoride transport experiments in the presence of valinomycin using DPPC vesicles** — DPPC vesicles prepared in 10 mM HEPES buffer containing 300 mM KF at pH 7.2 were suspended in 10 mM HEPES buffer containing 300 mM KGlc at pH 7.2 (4 mL).<sup>7,8</sup> After the signal of the voltage had stabilized (~30 s), the measurement was initiated using an F-ISE at 25 °C or 45 °C. At  $t = 0$ s, valinomycin (1  $\mu$ M) dissolved in DMSO was added to the external solution. At  $t = 30$ s, the potent transporter was added to the assay. At  $t = 450$ s, 20  $\mu$ L of a Triton X solution (20% Triton X-100 in water (v/v)) was added to lyse the vesicles triggering the complete release of the fluoride salt. The value corresponding to 100% fluoride efflux was recorded at  $t = 700$  s after lysing the vesicles.

**Chloride efflux in the presence of valinomycin** — This assay was adapted from a previous report.<sup>7</sup> The EYPC/Chol-LUVs prepared in 10 mM HEPES buffer containing 300 mM KCl at pH 7.2 were suspended in 10 mM HEPES buffer containing 300 mM KGlc at pH 7.2 (4 mL). After the voltage signal stabilized (~30 s), the measurement was initiated using a chloride-selective electrode (Cl-ISE). At  $t = 0$ s, valinomycin (1  $\mu$ M) dissolved in DMSO was added to the assay. At  $t = 30$ s, the synthetic transporters were added to the assay. At  $t = 450$ s, 20  $\mu$ L of a Triton X solution (20% Triton X-100 in water (v/v)) was added to lyse the vesicles triggering the complete release of the chloride salt. The 100% chloride efflux value was recorded at  $t = 700$  s

after lysing the vesicles. The resulting data were fitted to the Hill equation to get the  $EC_{50}$  concentration of the transporter.

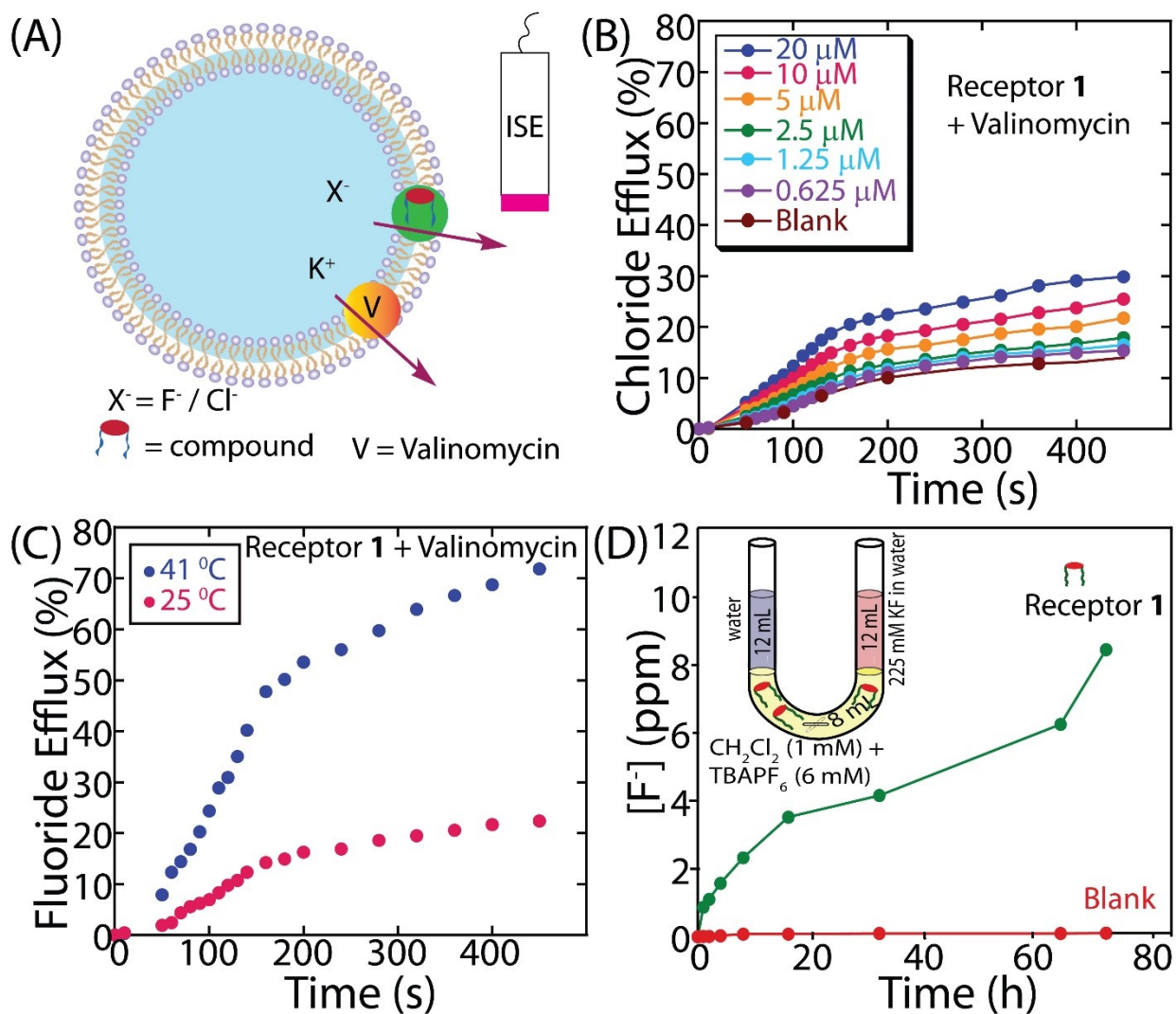


**Fig. S21.** Schematic representation of transmembrane anion transport activity studies using ion-selective electrode (A). Concentration-dependent valinomycin-coupled  $Cl^-$  ion efflux studies of receptor 1 in the presence of valinomycin (B). Temperature-dependent valinomycin-coupled  $F^-$  ion efflux studies of receptor 1 across DPPC bilayers (C). Time-dependent  $F^-$  ion transport study of receptor 1 across the U-tube (D).

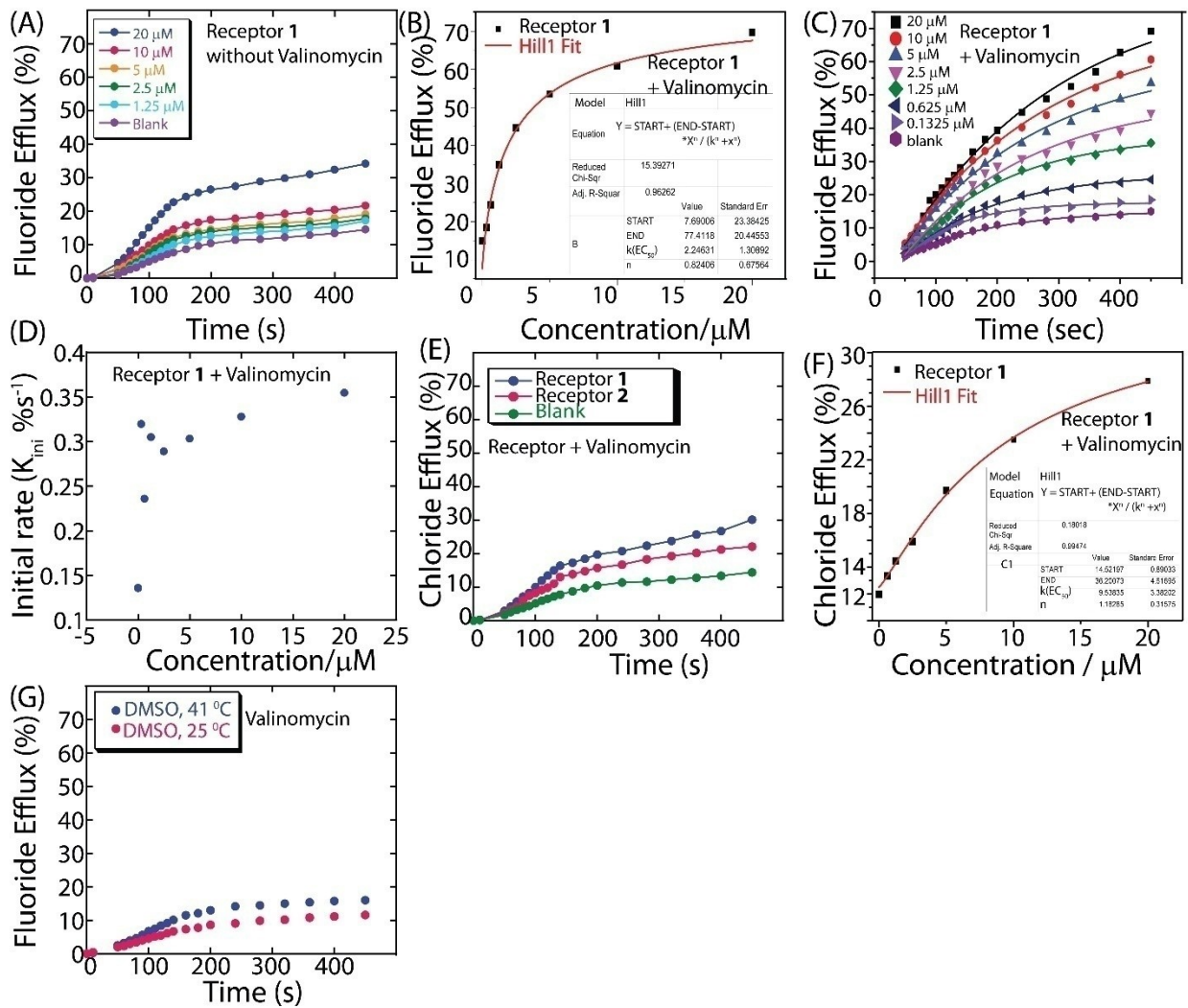


**Fig. S22.** Concentration-dependent  $F^-$  ion efflux studies of receptor **1** in the absence of valinomycin. LUVs were prepared in 10 mM HEPES buffer containing 300 mM KF at pH 7.2 and suspended in 10 mM HEPES buffer containing 300 mM KGlc at pH 7.2 (A). Analysis of valinomycin-coupled  $F^-$  ion efflux efficiency of receptor **1** (comparison of  $F^-$  ion efflux efficiency at 450 sec) (B). Calculation of the initial rate of valinomycin-coupled  $F^-$  ion efflux efficiency at different concentrations of receptor **1** (C and D). Concentration-dependent  $Cl^-$  ion efflux studies of receptor **1** in the presence of valinomycin. LUVs were prepared in 10 mM HEPES buffer containing 300 mM KCl at pH 7.2 and suspended in 10 mM HEPES buffer containing 300 mM KGlc at pH 7.2 (E). Analysis of valinomycin-coupled  $Cl^-$  ion efflux

efficiency of receptor 1 (comparison of Cl<sup>-</sup> ion efflux efficiency at 450 sec) (F). Control experiment for temperature-dependent DPPC assay (G).

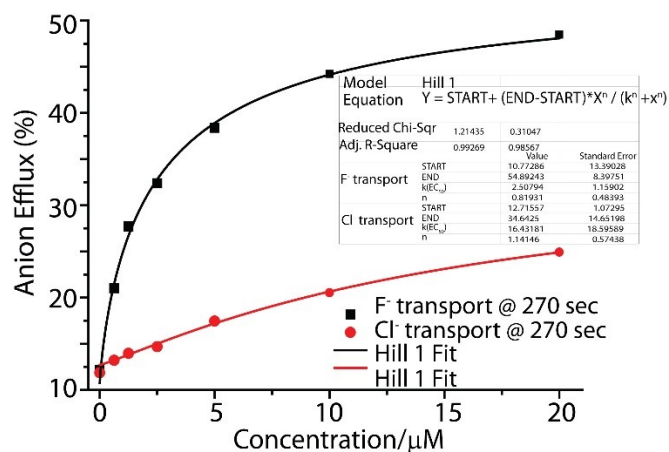


**Fig. S23.** Analysis of valinomycin-coupled F<sup>-</sup> and Cl<sup>-</sup> ion efflux efficiency of receptor 1 (comparison of Cl<sup>-</sup> ion efflux efficiency at 270 sec).

## References

1. Bruker, APEX2, SAINT and SADABS, BRUKER AXS, Inc. Madison, Wisconsin, USA, (2008).
2. G. M. Sheldrick, *Acta Cryst.*, 2008, **A64**, 112.
3. L. J. Farrugia, *J. Appl. Crystallogr.*, 2012, **45**, 849.
4. G. M. Sheldrick, *Acta Cryst.*, 2015, **C71**, 3.
5. A. L. Spek, *Acta Cryst.*, 2009, **D65**, 148.
6. L. J. Farrugia, *J. Appl. Crystallogr.*, 1997, **30**, 565.
7. G. Park, F. P. Gabbai, *Angew. Chem. Int. Ed.*, 2020, **59**, 5298.
8. N. Akhtar, O. Biswas, D. Manna, *Org. Biomol. Chem.*, 2021, **19**, 7446.